

PROCEEDINGS OF SPIE

SPIEDigitalLibrary.org/conference-proceedings-of-spie

Multiple piezo-patch energy harvesters on a thin plate with respective AC-DC conversion

Amirreza Aghakhani, Ipek Basdogan

Amirreza Aghakhani, Ipek Basdogan, "Multiple piezo-patch energy harvesters on a thin plate with respective AC-DC conversion," Proc. SPIE 10595, Active and Passive Smart Structures and Integrated Systems XII, 105951B (15 March 2018); doi: 10.1117/12.2296831

SPIE.

Event: SPIE Smart Structures and Materials + Nondestructive Evaluation and Health Monitoring, 2018, Denver, Colorado, United States

Multiple piezo-patch energy harvesters on a thin plate with respective AC-DC conversion

Amirreza Aghakhani*^a, Ipek Basdogan^a

^aDepartment of Mechanical Engineering, College of Engineering,
Koç University, Istanbul, 34450, Turkey;

ABSTRACT

Piezoelectric patch energy harvesters can be directly integrated to plate-like structures which are widely used in automotive, marine and aerospace applications, to convert vibrational energy to electrical energy. This paper presents two different AC-DC conversion techniques for multiple patch harvesters, namely single rectifier and respective rectifiers. The first case considers all the piezo-patches are connected in parallel to a single rectifier, whereas in the second case, each harvester is respectively rectified and then connected in parallel to a smoothing capacitor and a resistive load. The latter configuration of AC-DC conversion helps to avoid the electrical charge cancellation which is a problem with the multiple harvesters attached to different locations of the host plate surface. Equivalent circuit model of the multiple piezo-patch harvesters is developed in the SPICE software to simulate the electrical response. The system parameters are obtained from the modal analysis solution of the plate. Simulations of the voltage frequency response functions (FRFs) for the standard AC input – AC output case are conducted and validated by experimental data. Finally, for the AC input – DC output case, numerical simulation and experimental results of the power outputs of multiple piezo-patch harvesters with multiple AC-DC converters are obtained for a wide range of resistive loads and compared with the same array of harvesters connected to a single AC-DC converter.

Keywords: Piezoelectricity, energy harvesting, equivalent circuits, AC-DC conversion

1. INTRODUCTION

Piezoelectric energy harvesting research has advanced significantly over the past decade for powering small electronic components ^{1,2}. Among the various transduction mechanisms ranging from electrostatic ³, electromagnetic ⁴, magnetostrictive ⁵, piezoelectric ⁶ to electroactive and electrostrictive polymers ^{7,8}, piezoelectric transducers are the most used ones due to their high power density and voltage, which are comparable to some lithium-ion based batteries ⁹. Also, they can be easily manufactured and implemented at different scales ^{10,11}.

In the literature of piezoelectric energy harvesting, cantilevered beam harvesters have been the main focus of study by groups of researchers ^{11,12}. A variety of theoretical models such as single-degree-of-freedom model ¹³, Rayleigh-Ritz discretization model ¹⁴, and the closed-form distributed parameter model ¹⁵ were proposed to estimate the electrical outputs. Details of these mathematical modeling are summarized in ¹. Besides, finite-element modeling ¹⁶⁻¹⁸ and experimental tests ¹⁹ were performed by several other researchers to check the validity of the analytical models. Among the many studies on cantilever-based designs, only a few researchers have considered piezoelectric energy harvesting from the two-dimensional plate and shell structures. Piezoelectric patches bonded on thin plates enable compact energy harvesting without causing extra mass loading and occupying space. Moreover, cantilever plate designs usually possess a relatively large number of vibrational modes compared to the conventional cantilever beams, and also they are frequently utilized in aerospace, automotive and marine applications, which makes the patch-based energy harvesting convenient to apply and provide a wideband power harvesting.

For predicting the average power outputs of both cantilever beam and plate-like harvesters, mostly, a resistive load is used as a consumer part. However, in practical applications, stable DC signal is required for conveying the generated electrical power to the low-power electronic nodes or charging a storage component such as a battery or a supercapacitor. A standard AC-DC converter can provide a DC output at the resistive load, which consists of a full-wave bridge rectifier followed by a smoothing capacitor. Often as an extra stage, a DC-DC converter is used for the purpose of impedance matching to maximize the power flowing to the storage device ²⁰. The equivalent circuit model of single piezo-patch

energy harvester with nonlinear circuit elements has been recently developed by Bayik et al.²¹. The developed equivalent model can be analyzed via electronic circuit simulator (e.g., SPICE) which allows predicting the electrical outputs of the harvester with different circuit interfaces. It also accounts for two-way electromechanical coupling of the piezoelectric patch and the vibrating plate as well as multiple vibration modes of the plate. Analytical formulations expressing the steady-state DC voltage output of the array of beam harvesters were presented by Lien and Shu²² who employed the energy balance approach and equivalent impedance of the harvesting circuit to derive the closed-form expression. Later, they²³ analyzed the same array of harvesters, while each harvester is connected independently to a rectifier and then connected to a smoothing capacitor and resistive load. However, in both studies, derivations are based on SDOF modeling. More recently, Aghakhani et. al^{24,25} have presented both equivalent circuit modeling and analytical distributed-parameter expressions for DC electrical output of the multiple piezo-patch harvesters attached to a thin plate.

This paper presents numerical simulations and experimentally validated results for multiple piezo-patch harvesters connected to two different AC-DC converter circuits: single rectifier and multiple rectifiers. The single rectifier circuit is usually used for providing DC voltage, however, the second circuit with multiple rectifiers has the benefits of avoiding charge cancellation, which occurs due to the opposite signs of strain distribution under the piezoelectric patches. Yet, one drawback of such circuit configuration on the electrical output is the added voltage drops from the nonlinear diodes, which can be ameliorated by choosing low-loss rectifiers. It is expected that when each piezo-patch is respectively rectified, more electrical power is generated than the single rectification case. In the following section, a multi-mode equivalent circuit model of multiple piezo-patch harvesters integrated to a thin plate is developed into SPICE software. Equivalent circuit parameters of the multiple harvesters are obtained through the analogy with the governing electromechanical equations of piezo-patch harvesters and then are updated using the experimentally obtained voltage FRFs. AC input – AC output and AC input – DC output problems are explored numerically and verified with experiment results. SPICE simulations and experimental results for DC electrical outputs of the harvester with single rectifier circuit are reported for a wide range of resistive loads. Comparison of DC voltage and average power outputs across the optimum resistive load for both single and multiple rectifier circuit types are also shown for the first six vibration modes.

2. ANALYTICAL DISTRIBUTED-PARAMETER MODELLING

Figure 1 presents the schematic of multiple piezo-patch energy harvesters bonded on a thin plate and connected in parallel to an electrical impedance. Length and width of the host plate are a and b respectively, the thickness is denoted by h_s and assumed to be much smaller than other dimensions so that the effects of normal stress in the thickness direction and the corresponding transverse shear stresses are ignored (based on Kirchhoff plate theory). A transverse point force $f(t)$ is exciting the plate at the position coordinates (x_0, y_0) . Note that hereafter, the subscripts \bar{s} and \bar{p} indicate the parameters regarding the host structure and piezoelectric patches respectively. The total number of patch harvesters is given by $n_{\bar{p}}$, and each piezoceramic patch placed on the plate is located with two corners at $(x_{k,1}, y_{k,1})$ and $(x_{k,2}, y_{k,2})$, with $k = 1, 2, \dots, n_{\bar{p}}$. The thickness of the k -th patch is shown by $(h_{\bar{p}})_k$ and the polarization is assumed to be in the thickness direction.

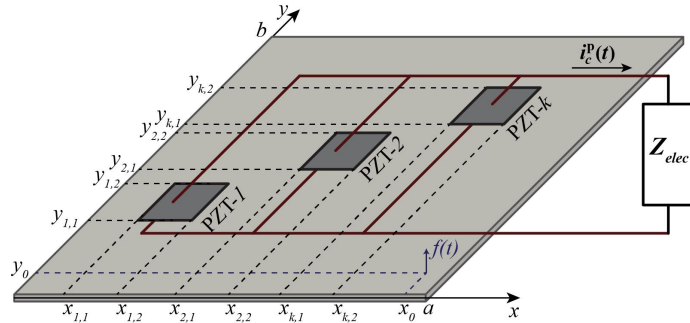


Figure 1. Multiple piezo-patch energy harvesters (in parallel configuration) bonded on a thin plate and connected to an electrical circuit with equivalent impedance Z_{elec}

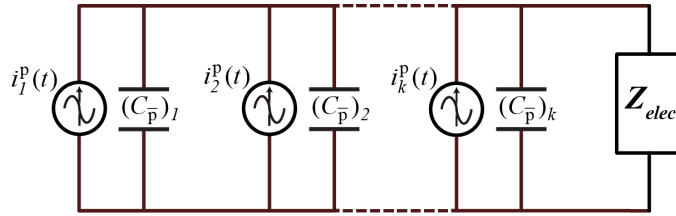


Figure 2. Electrical representation of multiple piezo-patch harvesters connected in parallel to an electrical impedance

Following the modal analysis procedure for the thin two-dimensional structure²⁶, governing electromechanically coupled equations of the plate in modal coordinates are given as

$$\begin{aligned} \frac{d^2\eta_{mn}^p(t)}{dt^2} + 2\zeta_{mn}\omega_{mn} \frac{d\eta_{mn}^p(t)}{dt} \\ + \omega_{mn}^2 \eta_{mn}^p(t) - v^p(t) \sum_{k=1}^{n_p} (\tilde{\theta}_{mn})_k = f_{mn}(t) \end{aligned} \quad (1)$$

$$\sum_{k=1}^{n_p} \sum_{n=1}^{\infty} \sum_{m=1}^{\infty} (\tilde{\theta}_{mn})_k \frac{d\eta_{mn}^p(t)}{dt} + \frac{dv^p(t)}{dt} \sum_{k=1}^{n_p} (C_{\bar{p}})_k + i_c^p(t) = 0 \quad (2)$$

where $\eta_{mn}^p(t)$, ω_{mn} and ζ_{mn} are the corresponding modal coordinate, undamped natural frequency and modal damping ratio for the mn -th vibration mode of the plate. The equivalent capacitance for the k -th piezo-patch is expressed as

$(C_{\bar{p}})_k = (\bar{\varepsilon}_{33}^S)_k \frac{(l_{\bar{p}})_k (w_{\bar{p}})_k}{(h_{\bar{p}})_k}$. The patch dimension parameters $(l_{\bar{p}})_k$, $(w_{\bar{p}})_k$ and $(h_{\bar{p}})_k$ are the length, width, and

thickness of the k th patch harvester, respectively, and the permittivity of the k th piezo-patch at constant strain is denoted by $(\bar{\varepsilon}_{33}^S)_k$. The electromechanical coupling term $(\tilde{\theta}_{mn})_k$ and the modal forcing input $f_{mn}(t)$ are as follow

$$(\tilde{\theta}_{mn})_k = \theta_k \int_{y_{k,1}}^{y_{k,2}} \int_{x_{k,1}}^{x_{k,2}} \left[\frac{\partial^2 \phi_{mn}(x,y)}{\partial x^2} + \frac{\partial^2 \phi_{mn}(x,y)}{\partial y^2} \right] dx dy \quad (3)$$

$$f_{mn}(t) = f(t) \phi_{mn}(x_0, y_0) \quad (4)$$

Here, $\phi_{mn}(x,y)$ is the mass-normalized mode shape of the plate at the mn -th vibration mode. The electromechanical term θ_k for the k th patch harvester is given by $\theta_k = (h_{pc})_k (\bar{e}_{31})_k$, which is the product of effective piezoelectric constant $(\bar{e}_{31})_k$ and reference distance $(h_{pc})_k$, which for the k -th patch is defined as the distance from the center layer of k th piezo-patch to center layer of the plate. It should be noted that since the piezo-patches are connected in parallel, their voltage across the electrodes is equal, that is $v^p = v_k^p(t)$. Finally, the electrical current flowing in the direction of the electrical impedance Z_{elec} is indicated by $i_c^p(t)$.

3. EQUIVALENT CIRCUIT MODELING

The analytical distributed-parameter model of the plate with single/multiple piezo-patch energy harvesters is capable of predicting the power output when the interface circuit is a simple resistance²⁶. Although those models explore the fundamental behavior of the electromechanical system, they ignore the dynamics of more sophisticated circuits that are utilized to produce stable DC voltage signal and transfer it to the end devices such as batteries or sensor nodes. To this end, this section introduces the equivalent circuit model that is developed into numerical simulation software SPICE, to accurately predict the dynamics of the harvesting circuit and its effect on the mechanical part. For the details of obtaining the equivalent circuit parameter for the piezo-patch harvester both from analytical and finite-element model, the reader is referred to²¹. System parameters identified for the single piezo-patch harvesters is extended to the case of multiple piezo-patch harvesters in this study, by taking into account the full electromechanical coupling behavior of piezo-patches and the host plate.

Figure 3 shows the equivalent circuit model for the k -th piezo-patch harvester, where the dependent current source constitutes of multiple secondary-order circuits, which represent the multiple vibration modes. By repeating this substitution for $k = 1, 2, \dots, n_{\bar{p}}$ in Figure 2, and constructing these equivalent circuits along with an interface circuit in SPICE, transient simulations can be performed to estimate the electrical outputs.

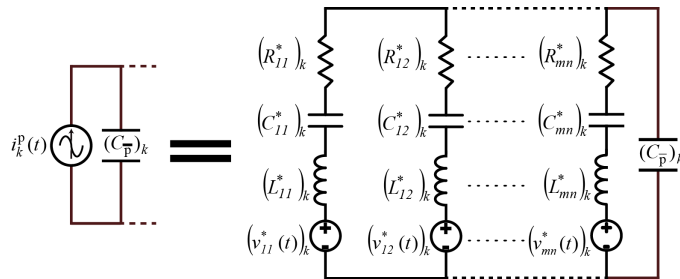


Figure 3. Equivalent circuit modeling for the k -th piezo-patch harvester in parallel configuration by accounting for multiple vibration modes (a total of $m \times n$ modes)

According to the analogy between the analytical distributed-parameter expression (Eq. (1) and Eq. (2)) and the equivalent circuit model shown in Figure 3, system parameters are obtained and summarized in Table 1. It's worth pointing out the differences in the equivalent parameters of the mechanical part for single versus multiple piezo-patch harvesters integrated into a thin plate. In the single harvester case, for each vibrational mode, there is only single

coupling term $\tilde{\theta}_{mn}$ in the elements of mechanical impedance where the terms are defined as $R_{mn}^* = \frac{2\zeta_{mn}\omega_{mn}}{\tilde{\theta}_{mn}^2}$,

$L_{mn}^* = \frac{1}{\tilde{\theta}_{mn}^2}$, $C_{mn}^* = \frac{\tilde{\theta}_{mn}^2}{\omega_{mn}^2}$ and the equivalent voltage source as $v_{mn}^*(t) = -\frac{f_{mn}(t)}{\tilde{\theta}_{mn}}$. However, in the case of multiple

harvesters, the system parameters of the single harvester cannot be simply mapped into the k -th piezo-patch harvester. Therefore, the system parameters for the parallel configuration of MPPHs are modified as given in Table 1, which accounts for the backward coupling effect of all the piezoelectric patches on the host plate. They also agree with mechanical Eq. (1) as well as electrical Eq. (2).

Table 1. Analogy between electrical and mechanical domains of multiple piezo-patch energy harvesters integrated to a thin plate

Equivalent circuit parameters	Mechanical counterparts
Voltage source: $(v_{mn}^*(t))_k$	$-\frac{1}{\sum_{k=1}^{n_p} (\tilde{\theta}_{mn})_k} f_{mn}(t)$
Electrical current: $(i_{mn}^*(t))_k$	$-(\tilde{\theta}_{mn})_k \dot{\eta}_{mn}^p(t)$
Inductance: $(L_{mn}^*)_k$	$\frac{1}{(\tilde{\theta}_{mn})_k \sum_{k=1}^{n_p} (\tilde{\theta}_{mn})_k}$
Resistance: $(R_{mn}^*)_k$	$\frac{2\zeta_{mn}\omega_{mn}}{(\tilde{\theta}_{mn})_k \sum_{k=1}^{n_p} (\tilde{\theta}_{mn})_k}$
Capacitance: $(C_{mn}^*)_k$	$\frac{(\tilde{\theta}_{mn})_k \sum_{k=1}^{n_p} (\tilde{\theta}_{mn})_k}{\omega_{mn}^2}$

4. AC-DC CONVERTER CIRCUITS

In this section, two AC-DC converter circuit models are introduced. In the first model, all the piezo-patches are connected in parallel to a full-wave rectifier followed by a smoothing capacitor and a resistive load. However, in the second model, each piezo-patch is respectively connected to a rectifier, and all the rectifiers are then connected in parallel to a smoothing capacitor and load resistance.

Figures 4 and 5 show schematics for the single rectifier model and multiple rectifiers models, respectively. It should be noted that a low-pass filter, consisting of R_{filter} and C_{filter} is placed between the smoothing capacitor and the resistive load, in order to reduce the amount of ripple and high-frequency noises.

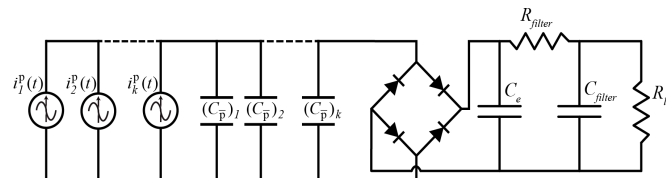


Figure 4. Single rectifier model

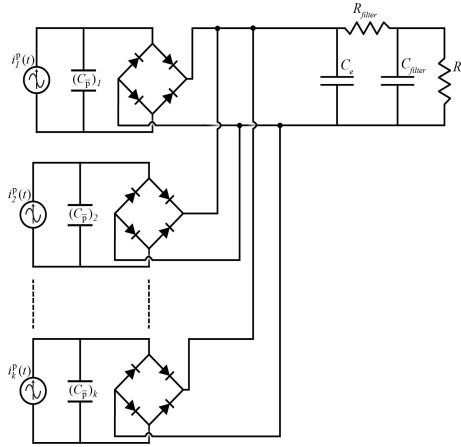


Figure 5.Multiple rectifiers model

5. EXPERIMENTAL SETUP

This section introduces the experimental setup used for analyzing the harvesting performance of multiple piezo-patch configurations. The experimental setup used for system identification and experimental tests is shown in Figure 6. Resonance frequencies and damping ratios are experimentally identified and used for updating the equivalent system parameters.

A fully clamped rectangular aluminum plate is used a thin plate. The transversely isotropic piezoceramic patches (T105-A4E-602 manufactured by Piezo Systems, Inc.) are employed as piezo-patch harvesters bonded on the aluminum plate. The geometric, material, and electroelastic properties of the plate and the piezo-patch harvesters are given in Table 2. Two piezo-patches (indicated by PZT-1 and PZT-2) are attached on the front surface of the aluminum plate as shown in Figure 4. The attachment regions on the aluminum plate are electrically isolated with 3M Scotch 1601 Insulating Spray. The center of the PZT-1 is located at 0.174 and 0.270 m away from the bottom left corner of the plate, whereas the center of the PZT-2 is at 0.275 and 0.164 m away from the bottom left corner. For the AC input – AC output case, the aluminum plate is excited by a linear sine sweep signal over the bandwidth of 1–260 Hz through a modal shaker during the experimental frequency response measurements. For AC input – DC output case, excitation frequency is linearly swept up and down around each resonance frequency at the rate of 0.02 Hz/s. The sweep rate is set in a way to allow enough charge time for the smoothing capacitor. The shaker's rod is attached to 0.085 and 0.085 m away from the right bottom of the plate. The dynamic point force acting on the plate is measured by a force transducer (PCB 208C02) which is placed between the shaker's rod and the plate surface. A data acquisition system is set to record and analyze the signals coming from the force transducer, and the voltage across the resistive load.



Figure 6. Experimental setup: (a) PZT-1, (b) PZT-2, (c) aluminum plate, (d) clamping frame, (e) electrical circuit (f) shaker with a force transducer, (g) data acquisition unit, and (h) signal generator.

Table 2. Geometric, material and electroelastic properties

Property	Aluminum	Piezoceramic
Length (mm)	580	72.4
Width (mm)	535	72.4
Thickness (mm)	1.9	0.267
Young's modulus (GPa)	65.1	66
Mass density (kg m^{-3})	2575	7800
Piezoelectric constant $d_{31}(\text{pm V}^{-1})$	-	-190
Permittivity constant $\bar{\epsilon}_{33}^S$ (nF m^{-1})	-	10.38

6. EXPERIMENTAL AND NUMERICAL RESULTS

In the numerical simulations, an equivalent circuit model of the multiple piezo-patch harvesters (shown in Figure 3) is developed in SPICE software. Then, harmonic transverse excitation tests are conducted using the experimental setup for different case studies. In the following, AC input – AC output and AC input – DC output cases are investigated, where in both cases, numerical and experimental results are compared.

6.1. AC input – AC output case

Here, the electrical impedance Z_{elec} as shown in Figure 1 is equal to a resistive load R_L . Equivalent system parameters given in Table 1 can be obtained from the analytical solution of harvester²¹. Although the analytical model predicts the modal behavior of the system, it cannot precisely predict the resonance frequencies and the other system parameters. Therefore, to obtain an accurate equivalent model, resonance frequencies, and modal damping ratios are extracted from the voltage FRFs obtained through experimental studies. Figure 7 shows the comparison of experimental and two numerical voltage FRFs for the short-circuit condition, where the resistive load is selected as 100Ω . In the SPICE simulation results (shown with blue line), it is assumed that system parameters are purely obtained from the analytical model. Whereas, in the second numeric result (dashed red line), system parameters are updated through system identification technique. It is clear that updated system parameters can accurately fit the vibration modes in the experiment result. From now on, the updated system parameters are used for the equivalent circuit model.

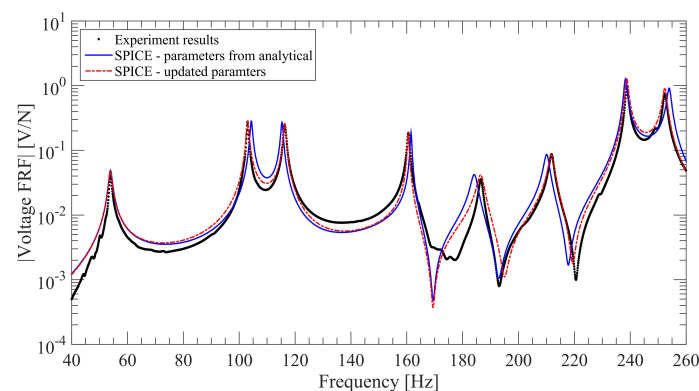


Figure 7. Comparison of experimental and numerical voltage FRFs for the short-circuited case ($R_L = 100\Omega$)

6.2. AC input – DC output case

In this section, two cases of AC-DC circuit configurations are analyzed for converting the AC voltage to stable DC voltage. The first case is the single standard AC-DC converter connected to the array of piezo-patches, and the second case considers each piezo-patch to be connected independently to a rectifier. In the experimental tests, for reducing the ripple and unwanted high-frequency noises, an extra low-pass filter is added to the harvesting circuit as shown in Figures 4 and 5. Note that for the AC input – DC output experiments, the inevitable ripple in the voltage and current output depend directly on the output time constant, that is the product of resistive load and a smoothing capacitor $R_l C_e$. It means that for a small amount of ripple, a large value of the time constant, $R_l C_e$, should be chosen. Additionally, frequency sweep rate must be chosen with respect to an inverse proportion of time constant so that the capacitor is fully charged. Hence, to avoid lengthy experiment tests, the output time constant is set to 0.1 seconds, which is about ten times the period of system excitation at the first vibration mode. That is, for the load resistance values ranging from 100Ω to $1M\Omega$, the smoothing capacitor values change from $1mF$ to $100nF$. For both SPICE simulations and experiments, commercially available Schottky diode BAT85 is used for the single/multiple full-wave rectifier circuits due to its low forward voltage drop and fast switching performance²⁷. The BAT85 diode parameters used in the SPICE software are given in Table 3.

Table 3. SPICE parameters for the BAT85 diodes in the rectifier circuit

Name	Value
IS (Saturation current)	207.6 nA
N (Emission coefficient, 1 to 2)	1.023
BV (Reverse breakdown voltage)	33 V
IBV (Reverse breakdown current)	10 μ A
RS (Parasitic resistance)	2.326 Ω
CJO (Zero-bias junction capacitance)	12.1 pF
VJ (Junction potential)	131.9 mV
M (Junction grading coefficient)	0.2904
EG (Activation energy)	0.69 eV
XTI (IS temperature exponent)	2

Figure 8 presents the comparison of SPICE simulation and the experimental results for DC voltage and power outputs across the various load resistances (100Ω to $1M\Omega$) under 1N harmonic force excitation at the first vibration mode. The electrical circuit, in this case, is a single rectifier as shown in Figure 4. Numerical results are shown to be in a good agreement with experiment results. From the average power results in Figure 8, the optimum resistive load for maximum power harvesting is estimated to be around $R_l = 5.56 k\Omega$. The short-circuit resonance frequency is also around 54.1 Hz.

The next set of experiments and numerical simulations are performed for comparing the performance of single and multiple rectifier circuits. For the rest of this study, all the energy harvesting tests are conducted with the optimum load resistance. As mentioned previously, in the single rectification case, the inevitable charge cancellation of piezoelectric patches causes low power generation. For a full analysis of strain distribution under the multiple piezo-patches, the reader is referred to²⁶.

Figures 9 and 10, present the comparison of DC voltage and power amplitudes of the multiple piezo-patch energy harvesters, for the single and multiple rectification cases. Experiment results, marked with (a) are compared against the SPICE simulation results, which are marked with (b). It is evident that after second vibration mode, both DC voltage and power output level are lower in the multiple piezo-patch harvesters with single rectifier circuit, which indicates the existence of charge cancellation in higher vibration modes. Especially in modes 5 and 6, DC voltage and power amplitudes are almost zero, when all the piezo-patches are rectified with single AC-DC converter. Note that, all the

excitations are conducted with 1 N point force. The numerical predictions agree well with the experimental data for the first six vibration modes as can be observed in Figures 9 and 10.

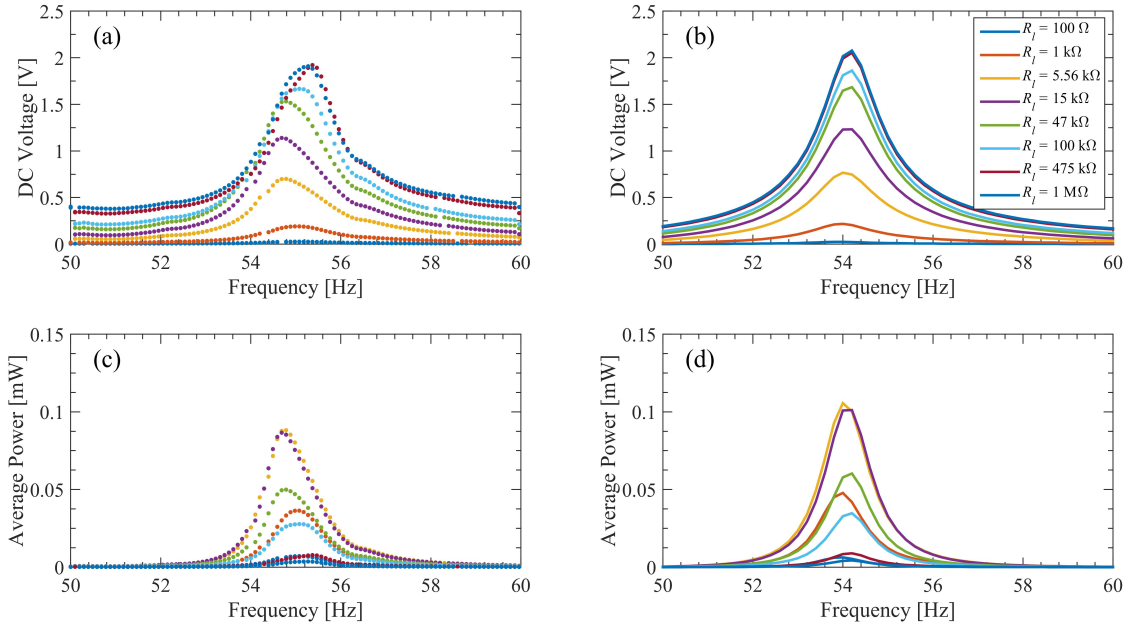


Figure 8. Variations of DC voltage and average power amplitudes of multiple piezo-patch harvesters (single rectification case) with resistive load at the first vibration mode: experiments are shown with dot markers in (a) and (c), and SPICE simulations are plotted with solid lines in (b) and (d)

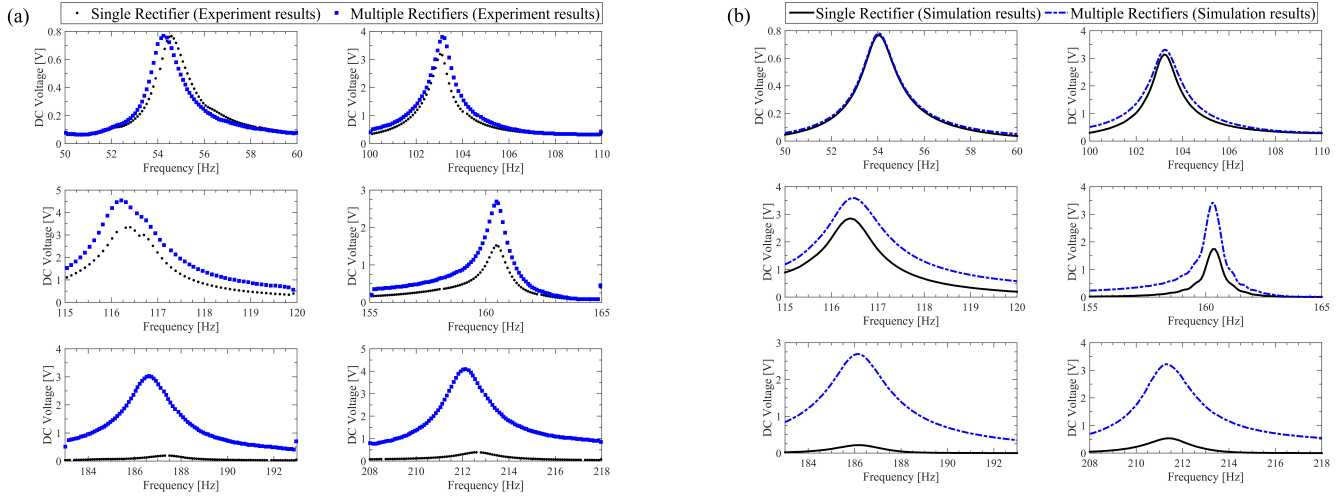


Figure 9. Comparison of DC voltage output for cases of multiple piezo-patch harvesters connected to single rectifier and multiple rectifier circuits: (a) experiment results (b) SPICE simulation results

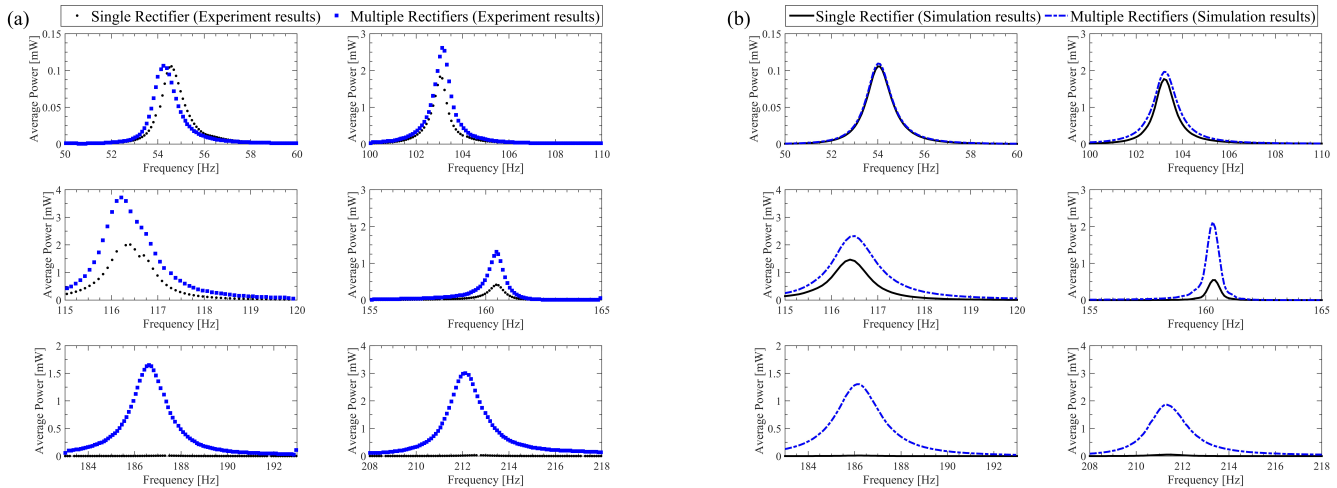


Figure 10. Comparison of average power output for cases of multiple piezo-patch harvesters connected to single rectifier and multiple rectifier circuits at the first six vibration modes: (a) experiment results (b) SPICE simulation results

7. CONCLUSION

This study presents the numerical modeling and experimental validation of multiple piezo-patch harvesters integrated into a thin plate can be with two AC-DC conversion mechanism. The multi-mode equivalent circuit model of the energy harvesting system, was developed in SPICE software. Equivalent circuit parameters were obtained analytically from the modal analysis solution and then updated through experimental voltage FRFs of the short-circuit condition. Then, using the equivalent circuit parameters, transient simulations were conducted in the AC input – DC output case with single electrical rectification for a wide range of resistance load values and validated experimentally. In the last section, DC electrical outputs of the multiple piezo-patches with multiple rectifiers circuit, where each piezo-patch is respectively rectified, was compared with those of the single rectifier circuit. Steady-state DC electrical responses were investigated for the optimum resistive load for the first six modes of the plate. In both numerical and experimental results, it was shown that at higher vibration modes, due to the charge cancellation, use of single AC-DC converter results in lower power harvesting. Although the use of multiple rectifiers may create an electrical loss, it's been shown that for the case of multiple piezo-patch harvesters, they are far more advantageous than single rectifier circuit. The experimental and numerical results presented in this article, highlight the effective broadband energy harvesting on thin plates using the multiple piezo-patches when the AC-DC converter circuit is carefully chosen.

REFERENCES

- [1] Erturk, A. and Inman, D. J., [Piezoelectric Energy Harvesting], John Wiley & Sons, Ltd, Chichester, UK (2011).
- [2] Harvesting, E., [Advances in Energy Harvesting Methods], Springer New York, New York, NY (2013).
- [3] Torres, E. O. and Rincón-Mora, G. A., “Electrostatic energy-harvesting and battery-charging CMOS system prototype,” IEEE Transactions on Circuits and Systems I: Regular Papers **56**(9), 1938–1948 (2009).
- [4] Beeby, S. P. and O’Donnell, T., “Electromagnetic Energy Harvesting,” [Energy Harvesting Technologies], Springer US, Boston, MA, 129–161 (2009).
- [5] Wang, L. and Yuan, F. G., “Vibration energy harvesting by magnetostrictive material,” Smart Materials and Structures **17**(4), 45009 (2008).
- [6] Priya, S., “Advances in energy harvesting using low profile piezoelectric transducers,” Journal of Electroceramics **19**(1), 167–184 (2007).
- [7] Ren, K., Liu, Y., Hofmann, H., Zhang, Q. M. and Blottman, J., “An active energy harvesting scheme with an

- electroactive polymer," Applied Physics Letters **91**(13), 132910 (2007).
- [8] Yiming Liu, Kai Liang Ren, Hofmann, H. F. and Qiming Zhang., "Investigation of electrostrictive polymers for energy harvesting," IEEE Transactions on Ultrasonics, Ferroelectrics and Frequency Control **52**(12), 2411–2417 (2005).
- [9] Cook-Chennault, K. A., Thambi, N., Bitetto, M. A. and Hameyie, E. B., "Piezoelectric Energy Harvesting," Bulletin of Science, Technology & Society **28**(6), 496–509 (2008).
- [10] Cook-Chennault, K. A., Thambi, N. and Sastry, A. M., "Powering MEMS portable devices—a review of non-regenerative and regenerative power supply systems with special emphasis on piezoelectric energy harvesting systems," Smart Materials and Structures **17**(4), 43001 (2008).
- [11] Anton, S. R. and Sodano, H. A., "A review of power harvesting using piezoelectric materials (2003-2006)," Smart Materials & Structures **16**(3), R1–R21 (2007).
- [12] Friswell, M. I. and Adhikari, S., "Sensor shape design for piezoelectric cantilever beams to harvest vibration energy," Journal of Applied Physics **108**(1), 14901 (2010).
- [13] Roundy, S. and Wright, P. K., "A piezoelectric vibration based generator for wireless electronics," Smart Materials and Structures **13**(5), 1131–1142 (2004).
- [14] Sodano, H. A., Park, G. and Inman, D. J., "Estimation of electric charge output for piezoelectric energy harvesting," Strain **40**(2), 49–58 (2004).
- [15] Erturk, A. and Inman, D. J., "A Distributed Parameter Electromechanical Model for Cantilevered Piezoelectric Energy Harvesters," Journal of Vibration and Acoustics **130**(4), 41002 (2008).
- [16] Yang, Y. and Tang, L., "Equivalent Circuit Modeling of Piezoelectric Energy Harvesters," Journal of Intelligent Material Systems and Structures **20**(18), 2223–2235 (2009).
- [17] Elvin, N. G. and Elvin, A. A., "A Coupled Finite Element--Circuit Simulation Model for Analyzing Piezoelectric Energy Generators," Journal of Intelligent Material Systems and Structures **20**(5), 587–595 (2008).
- [18] Rupp, C. J., Evgrafov, A., Maute, K. and Dunn, M. L., "Design of Piezoelectric Energy Harvesting Systems: A Topology Optimization Approach Based on Multilayer Plates and Shells," Journal of Intelligent Material Systems and Structures **20**(16), 1923–1939 (2009).
- [19] Erturk, A. and Inman, D. J., "An experimentally validated bimorph cantilever model for piezoelectric energy harvesting from base excitations," Smart Materials and Structures **18**(2), 25009 (2009).
- [20] Ottman, G. K., Hofmann, H. F., Bhatt, A. C. and Lesieutre, G. A., "Adaptive piezoelectric energy harvesting circuit for wireless remote power supply," IEEE Transactions on Power Electronics **17**(5), 669–676 (2002).
- [21] Bayik, B., Aghakhani, A., Basdogan, I. and Erturk, A., "Equivalent circuit modeling of a piezo-patch energy harvester on a thin plate with AC – DC conversion," Smart Materials and Structures **25**(5), 55015 (2016).
- [22] Lien, I. C. and Shu, Y. C., "Array of piezoelectric energy harvesting by the equivalent impedance approach," Smart Materials and Structures **21**(8), 82001 (2012).
- [23] Lien, I. C. and Shu, Y. C., "Piezoelectric array of oscillators with respective electrical rectification," 10 April 2013, 868806, International Society for Optics and Photonics.
- [24] Aghakhani, A., Basdogan, I. and Erturk, A., "Multiple piezo-patch energy harvesters integrated to a thin plate with AC-DC conversion: analytical modeling and numerical validation," Proc. SPIE 9806, Smart Materials and Nondestructive Evaluation for Energy Systems 2016 **9806**, 98060C, International Society for Optics and Photonics (2016).
- [25] Aghakhani, A. and Basdogan, I., "Equivalent Impedance Electroelastic Modeling of Multiple Piezo-Patch Energy Harvesters on a Thin Plate with AC-DC Conversion," IEEE/ASME Transactions on Mechatronics **22**(4), 1575–1584 (2017).
- [26] Aridogan, U., Basdogan, I. and Erturk, A., "Multiple patch-based broadband piezoelectric energy harvesting on plate-based structures," Journal of Intelligent Material Systems and Structures **25**(14), 1664–1680 (2014).
- [27] Tiwari, R., Ryoo, K., Schlichting, A. and Garcia, E., "Extremely low-loss rectification methodology for low-power vibration energy harvesters," Smart Materials and Structures **22**(6), 62001 (2013).